

Growth and characterization of organic Nonlinear optical material: acenaphthene DL- malic acid (ADLMA)

G. SIVA, R. BHARATHIKANNAN*, B. MOHANBABU

Department of Physics, Sri Ramakrishna Mission Vidyalaya College of Arts and Science, India

Organic single crystals of nonlinear optical material Acenaphthene DL-malic acid (ADLMA) have been grown successfully by the slow evaporation solution growth technique. To begin with, solubility tests were carried out for two solvents such as acetone and chloroform-methanol. Among the two solvents, the solubility of ADLMA was found to be the highest in chloroform-methanol, so crystallization of ADLMA was done from its aqueous solution. The elemental percentage of the material was carried out CHN analysis. The crystalline nature of ADLMA crystal was confirmed by the powder X-ray diffraction study and diffraction peaks were indexed. Vibration modes of the functional groups were recognized and studied by recording a FTIR spectrum. The optical transparency range and absorption has been studied throughout UV-Vis-NIR spectroscopy. The second harmonic generation efficiency of the grown ADLMA crystal has been obtained by the Kurtz-Perry powder technique. The grown crystals were subjected to TG/DTA analysis. The dielectric activities of the title compound crystal was investigated and measuring the dielectric loss and dielectric constant properties. The photoluminescence spectrum was also studied.

(Received November 20, 2014; accepted February 10, 2016)

Keywords: NLO crystal, Slow evaporation, Thermal and Electrical studies

1. Introduction

The demand of ultrafast optical respond materials is getting momentum in the post launch era of fiber optic communication, internet data transition and optoelectronic sensors. Nonlinear optics provides such materials from their special properties such as noncentrosymmetry, inherent ultrafast response, birefringence, phase matching, frequency doubling, summing and difference frequency generation, optical switching etc., [1-6]. Many attempts are being carried out to synthesize such materials. Normally organic chromophores exhibit higher and faster nonlinearities than their inorganic counterparts. It is well known for organic materials, the large delocalization of π electrons induces electro-optic effects and produces large nonlinear optical responses [7]. One of the advantages in working with organic materials is that they permit one to fine tune the chemical structure of the material and get the desired nonlinear effect [8].

In the present work, such an attempt has been made to grow an organic crystal. An organic material has been synthesized by taking acenaphthene and DL-malic acid in 1:1 ratio. This synthesized material was grown as single crystals of acenaphthene DL-malic acid (ADLMA) using slow evaporation technique. All the relevant characteristic studies were carried out for the grown crystals and compared with pure acenaphthene crystals [9]. The SHG conversion efficiency of the grown crystals has been noticed 3.5 times that of standard NLO material, KDP. The optical, structural, thermal and electrical properties are analyzed and reported.

2. Experimental

2.1. Solubility studies

The growth of the bulk single crystals is mainly depending on the selection of solvents. As solubility is being the one of the major criteria to select a suitable solvent, the solubility test was carried out with different solvents. The chloroform-methanol 1:1 mixture and acetone were selected for this test and determined in the temperature ranges 30-45° C in steps of 5° C by gravimetric method. The solubility curves for chloroform-methanol (1:1) and acetone are shown in Fig.1. From the obtained data it was found that the solubility of ADLMA in chloroform-methanol (1:1) is higher than that of acetone. The title compound exhibits a positive solubility temperature gradient with good solubility in chloroform-methanol (1:1) solution, indicating the possibility of growing single crystals of ADLMA by slow evaporation method.

2.2. Materials synthesis

ADLMA was synthesized from acenaphthene and DL-malic acid which taken in the ratio of 1:1. The scheme.1 shows the reaction involved in material synthesis. The two reactants were prepared separately in chloroform and methanol and then mixed together. The resulting solution was stirred well for about one hour using a magnetic stirrer to ensure homogeneous solution. The stirred solution was filtered off using whatmann filter paper. The filtered solution was transferred to crystal growth vessels followed by slow evaporation at room temperature. Good

transparent crystals were obtained in a period of 10 days. The photograph of as grown crystals of ADLMA is shown in Fig.2.

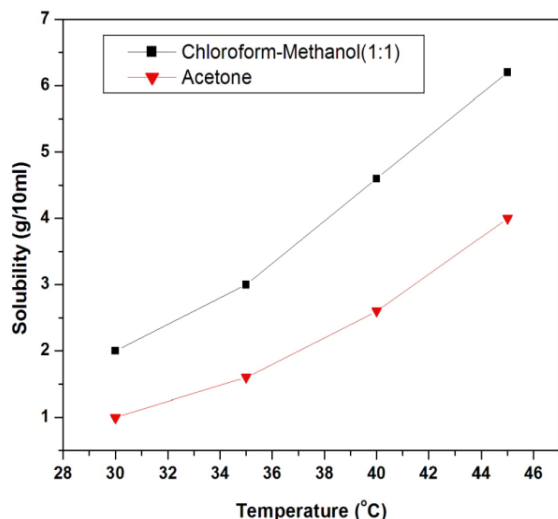


Fig. 1. Solubility curves of ADLMA crystal.

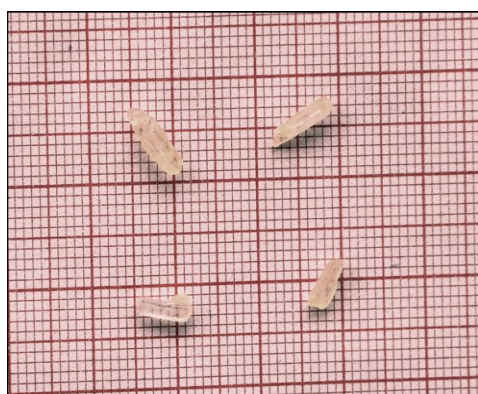
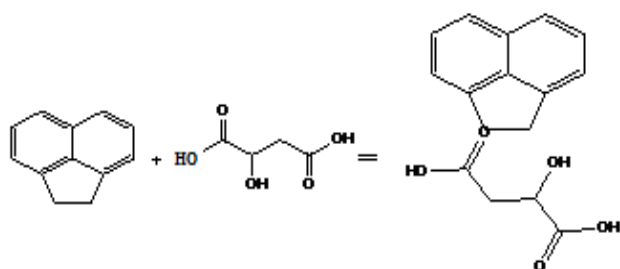


Fig. 2. Photograph of grown ADLMA single crystals.

Scheme 1. The reaction involved in material synthesis



Acenaphthene + DL-malic acid = Acenaphthene
DL-malic acid

2.3. Characterization

X-ray powder diffraction data for the ADLMA was taken by Bruker AXS D8 Advance Powder diffracting system of X-ray Radiation of wavelength 1.54059 \AA in the range 2θ which is scanned from 5° - 80° at room

temperature. Fourier transform infrared spectrum (FTIR) of ADLMA crystal was recorded in the range of $4000\text{-}400 \text{ cm}^{-1}$ employing a Perkin- Elmer spectrometer using KBr pellet technique. The UV-visible absorption and transmittance spectrum of ADLMA crystal was recorded using SYSTRONICS DOUBLE BEAM UV-Vis spectrophotometer in the wavelength range $200\text{-}1200 \text{ nm}$. The dielectric study of grown ADLMA single crystal was carried out using 3532-50 HIOKI LCR meter. The dimension of the used samples was $9 \times 9 \times 2 \text{ mm}^3$. To find out the melting point and phase transition of ADLMA, TG/DTA studies were performed with SDT Q600 V8.2 analyzer. Direct band gap energy was calculated from photoluminescence studies. Elemental composition percentage presents in ADLMA were done using Elementer vario EL III. The powder second harmonic generation output of the sample was measured by Nd-YAG laser.

3. Results and discussion

3.1. Elemental analysis

The chemical composition of the constituent elements present in ADLMA was verified through elemental analysis. The results of the theoretical and experimental elemental percentages are depicted in the table 1. The measured data are having good agreement with the theoretical values which indicate the presence of ADLMA crystal.

Table 1. Elemental analysis for ADLMA Chemical composition.

Element	Experimental value (%)	Theoretical value (%)
C	65.23	66.6
H	7.65	5.59

3.2. X-ray diffraction studies

The recorded powder X-ray diffraction spectrum of ADLMA is shown in Fig.3a and the reported XRD spectrum of acenaphthene (ANP) [9] is shown in Fig.3b. The experimental values of 2θ and d of ADLMA obtained from powder XRD spectrum and are compared with previous literature of acenaphthene, depicted in table 2. The values of 2θ and d of ADLMA are having good agreement with that of acenaphthene and with some additional peak around 21° . This additional information confirms the grown crystals are ADLMA. The sharp peaks and full-width at half maximum (FWHM) values confirms the grown crystal is good in crystallinity. From XRD spectral data, the microscopic structural parameters such as crystallite size, dislocation density and strain can be calculated.

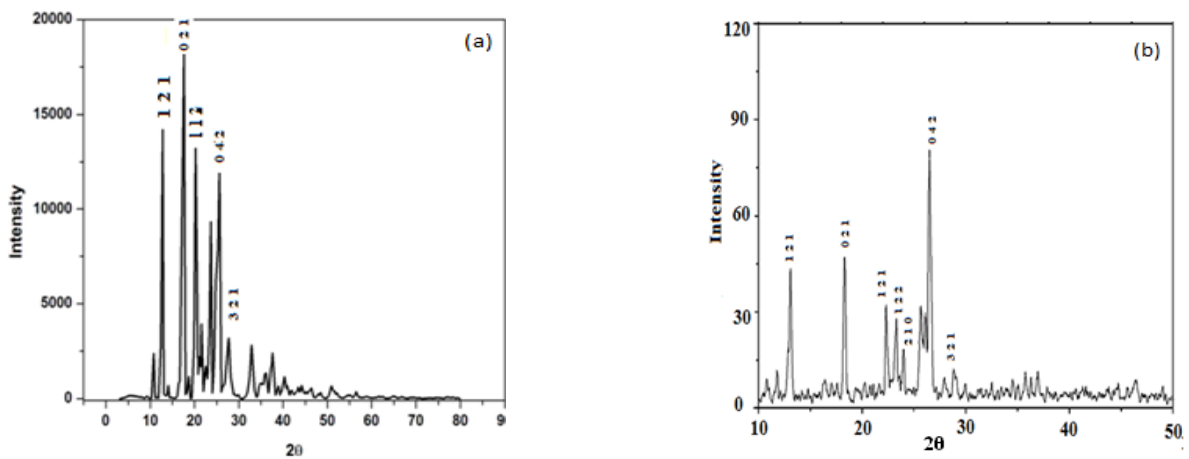


Fig. 3. Powder X-ray diffraction pattern of (a) ADLMA crystal and (b) ANP crystal.

The crystallite size (D) is calculated using Debye-Scherrer formula (1).

$$D = k\lambda/\beta\cos\theta \quad (1)$$

where, k is proportionality constant, approximately equal to unity, β the FWHM of the peak in radians (theoretically corrected from the instrumental broadening), λ is the wavelength of X-rays (1.5406 Å for CuK α) and θ is the Bragg's angle.

The dislocation density (δ) can be evaluated from Williamson and Smallman's formula,

$$\delta = 1/D^2 \text{ lines/m}^2 \quad (2)$$

and, micro strain (η) is determined using (3).

$$\eta = \beta\cos\theta/4 \quad (3)$$

For the prominent peak ($2\theta=17.544$), the crystallite size D is 36.5 nm, the dislocation density δ is 75.06×10^{13} lines/m 2 and the micro strain ϵ is equal to 0.00099.

3.3. FTIR spectral analysis

FTIR spectrum of ADLMA is depicted in Fig.4a and that of pure ANP [10] is shown in Fig.4b. Generally multiple weak bands are observed in the region 3000-3300 cm^{-1} for aromatic compounds, which are due to the stretching vibration of aromatic group C-H. The weak peak in FTIR spectrum at 2950 and 2940 cm^{-1} are due to CH stretching vibration of naphthalene ring present in ADLMA. The C-C stretching modes observed from 1600 to 900 cm^{-1} for ADLMA and ANP are in good agreement with the general appearance of C-C stretching modes. The naphthalene ring wagging starts below 938 cm^{-1} in case of ANP and that is at 1129 cm^{-1} in case of ADLMA. The modes appearing below 600 cm^{-1} are described to skeletal out of plane deformations or the torsional modes. Although this spectrum also carries similar features of that of ANP, there is distinct evidence for presence of DL-malic in the single crystals of ADLMA. The CH $_2$ stretching vibration observed at 2246 and 2112 cm^{-1} indicates the presence of DL-malic acid in ADLMA. The frequency assignments for ADLMA and ANP with various functional groups are presented in table 3.

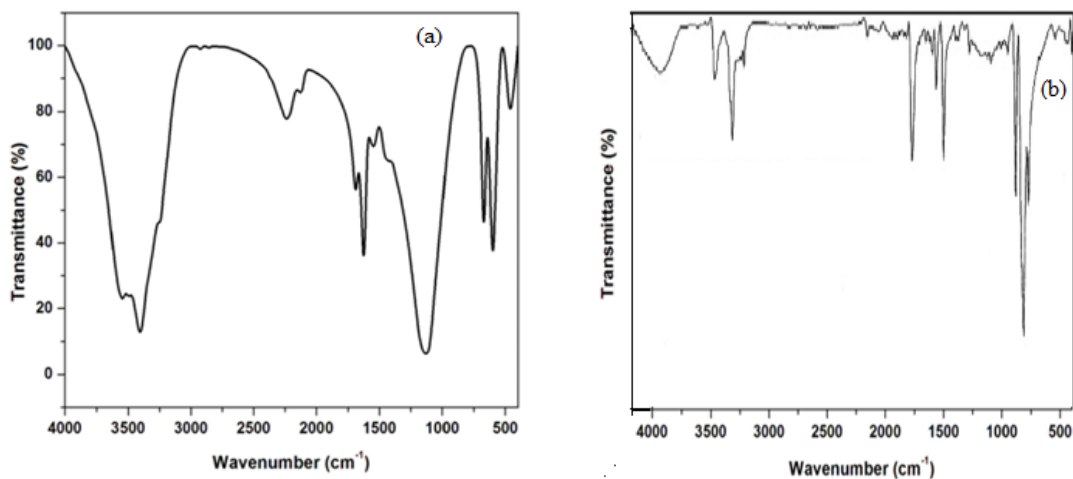


Fig. 4. FTIR spectrum of (a) ADLMA crystal and (b) ANP crystal.

Table 2. Powder XRD spectrum of ADLMA and ANP.

2θ degree	ADLMA (h k l)	ANP (h k l)
13	1 2 1	1 2 1
18	0 2 1	0 2 1
21	1 1 2	-----
23	1 2 1	1 2 1
26	0 4 2	0 4 2

Table 3. FT-IR spectral data of ADLMA and ANP.

Reported ANP in cm^{-1}	Experimental ADLMA in cm^{-1}	Assignments of dominant modes
—	3560	OH stretching vibration
—	3425	
—	3250	
2920	2950	C-H stretching vibration
2920	2940	
—	2246	CH ₂ stretching vibration
—	2112	
1601	1693	C-C stretching vibration
1601	1629	
938	1129	CH out plane N _p ring Wagging
745	680	skeletal out of plane or torsional modes deformation
541	598	

3.4. UV - visible spectrum

3.4.1. Absorption spectrum

The UV-visible spectrum gives limited information about the structure of the molecule because the absorption of UV and visible light involves the promotion of the electron from the ground state to higher energy states. The electronic absorption spectrum of the ADLMA crystal is depicted in Fig.5. The absorption peak at 295 nm is attributed to the charge transfer transition between donor and acceptor of the conjugated system. The absorption band arises due to the promotion of an electron from the

highest occupied orbital to the lowest unoccupied molecular orbital confirms the formation of charge transfer molecular complex. The spectrum indicates that there is no significant absorption in the visible and near infrared regions.

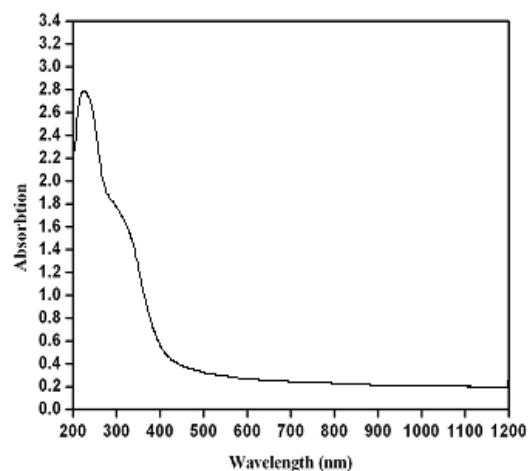


Fig. 5. UV- visible absorption spectrum of the ADLMA crystal.

3.4.2. Transmission spectrum

The spectrum of ADLMA and that of pure ANP are shown in Fig.6a & 6b respectively. From Fig.6b, it is understood, ANP crystal is transparent beyond 320 nm. In the case of grown ADLMA crystal the transparency starts at 340 nm with above 50% and beyond 500 nm it shows above 80% transparency are shown in Fig.6a. The shift of transparent window from 320 nm to 340 nm in ADLMA spectrum reveals that the presence of DL-malic acid groups in the ADLMA crystals. The peak at 350 nm is due to the n- π^* transition [11]. In crystals, the cracking and blackening impurities directly affect the optical transmittance. But no distortion was observed in the transmittance spectrum of grown crystal. The crystal is fully transparent in the entire visible region and near IR region, which indicates the optical quality and the suitability of the crystal, for various optical and electro-optic applications [12].

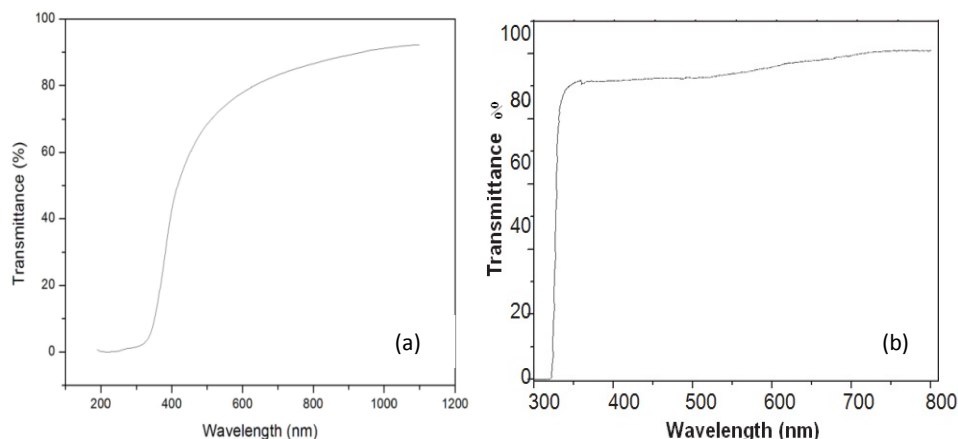


Fig. 6. UV-visible transmission spectrum of (a) ADLMA crystal and (b) ANP crystal.

3.5. Second harmonic generation

A preliminary study of the powder SHG property of as grown ADLMA crystals was examined through modified Kurtz and Perry powder technique [13]. In this method, powdered sample with an average crystallite sizes range 125 – 150 μm is tightly packed in a micro-capillary tube about 1.5 mm diameter. The sample was then subjected to the output of Q-switched Nd: YAG laser emitting a wavelength of 1064 nm with the power 2.1 mJ/P. The laser beam was well focused on the sample and the output signal of wavelength 532 nm was generated. This reduction in wavelength of input radiation by half confirms the second harmonic generation property. The green light intensity was registered by a photomultiplier tube and converted into an electrical signal. The SHG conversion efficiency was compared by the ratio of signal amplitude of the ADLMA sample to that of KDP signal amplitude recorded for the same input power. Present study confirmed high SHG efficiency of grown ADLMA crystal and its output was found to be 66 mV. The SHG studies of KDP, ADLMA and ANP were found to be 18mV, 66mV and 19mV respectively. It was found that ADLMA is three and half times greater than that of pure ANP value. It can be seen that the comparison of SHG Signal Energy Output listed in the table 4.

Table 4. Comparison of SHG signal energy output

Input power mJ/ pulse	KDP (mV)	ANP (mV)	ADLMA (mV)
2.1	18	19	66

3.6. Dielectric studies

Cut and polished samples of dimensions 9x9x2 mm³ were used for the dielectric measurement. Two opposite surfaces across the breadth of the sample were treated with good quality silver paste in order to obtain good ohmic contact. Using LCR meter, the capacitance of the crystal was measured from the frequency range 50Hz-2MHz at various temperatures. Fig.7 shows the plot of dielectric constant (ϵ_r) Vs frequency for temperature ranges 303K, 313K, 323K and 333K. The dielectric constant of the crystal was calculated using the relation

$$\epsilon_r = \frac{Cd}{\epsilon_0 A}$$

where, C_{crys} is the capacitance of the crystal, d is the thickness, ϵ_0 is free space permittivity and A is the area of the crystalline sample used. The dielectric constant has higher values in the lower frequency region and then it decreases with increasing frequency. The very high values of dielectric constant at low frequencies may be due to the presence of space charge, orientation, electronic, and ionic polarizations. The low value of dielectric constant at higher frequencies may be due to the loss of significance of these polarizations gradually. At higher frequency, the

defects have no long enough time to rearrange in response to the applied voltage, hence the capacitance decreases [14]. In accordance with Miller rule, the lower value of dielectric constant at higher frequencies has a suitable parameter for the enhancement of SHG coefficient [15]. The variation of dielectric loss with log frequency is shown in Fig.8. The low dielectric loss at high frequencies for the given sample suggests that sample possesses optical quality with lesser defects and this parameter play a vital role for the fabrication of nonlinear optical devices [16].

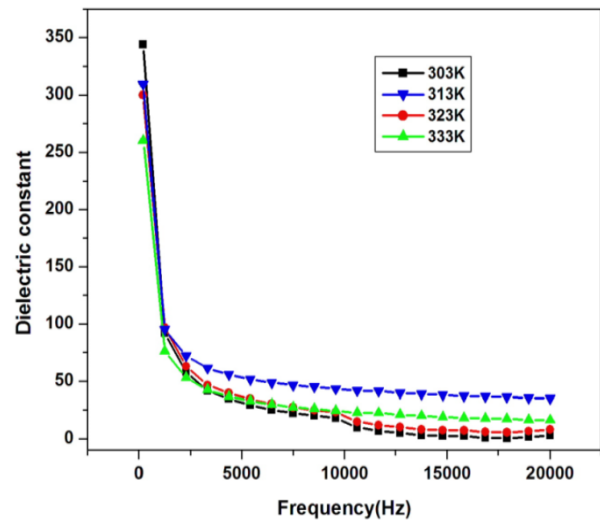


Fig. 7. Plot of dielectric constant (ϵ_r) vs. frequency of ADLMA crystal

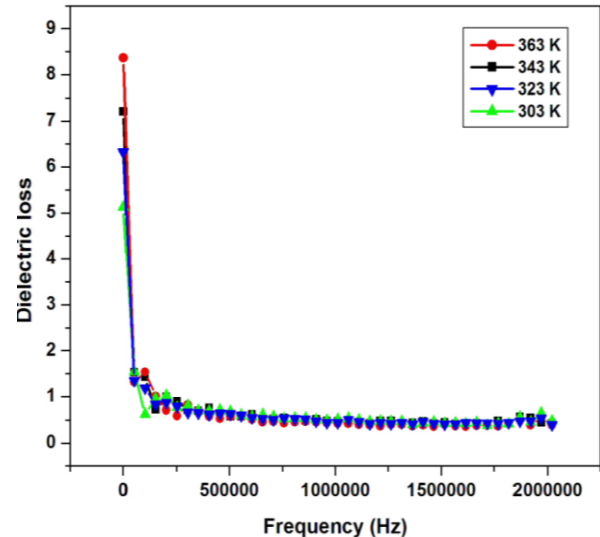


Fig. 8. Plot of dielectric loss vs. frequency of ADLMA crystal.

3.7. Thermal analysis

The thermo gravimetric spectrum of ADLMA crystal was recorded from 30^oC to 1000^oC at a heating rate of 10^oC/min in nitrogen gas atmosphere. Fig.9a and Fig.9b illustrate the TGA and DTA curves for the grown crystals

of ADLMA and pure ANP. TGA spectrum of ADLMA reveals that there are two stages of weight loss but for that of ANP is only one stage. There are two endothermic peaks observed in both the cases. The first endothermic peak represents the melting point of the crystal. The melting point of ANP and ADLMA are 98°C and 148°C respectively. The increase in melting point is due to the coordination of DL-malic acid with ANP, this suggests that it can be used for better thermal application than that of ANP.

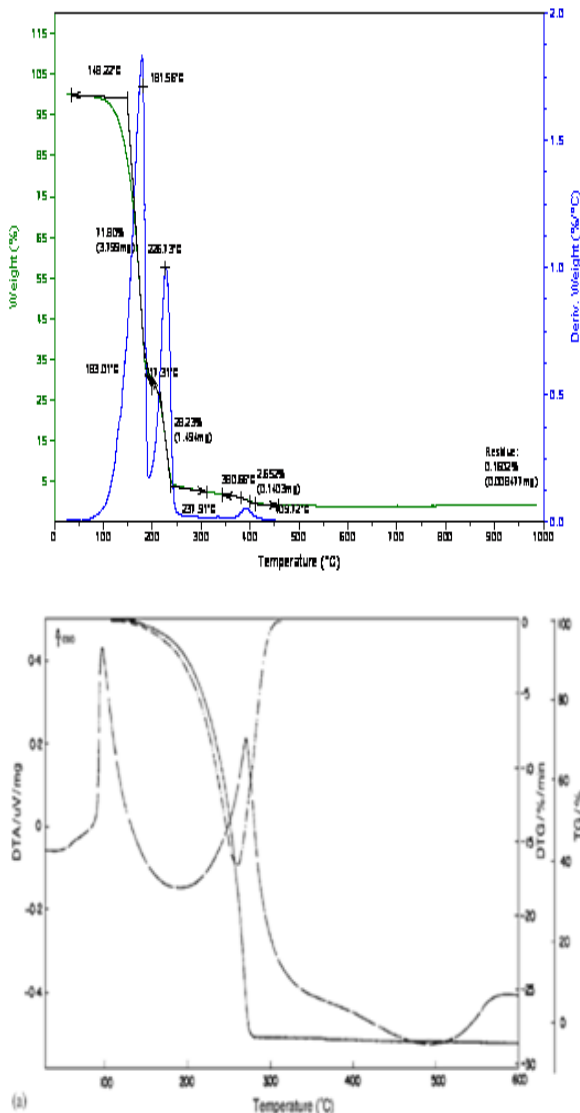


Fig. 9. TGA and DTA curves of grown (a) ADLMA crystal and (b) ANP crystal.

3.8. Photoluminescence

The intensity and spectral content of photoluminescence (PL) is a direct measure of various important material properties like band gap determination, impurity levels and defect detection. Emission spectrum gives the luminescence intensity as a function of wavelength while the wavelength of the exciting radiation

is kept constant. Emission spectra yields information about the position of activator levels, Fig.10 shows the emission spectrum of ADLMA crystal. Two emission peaks are observed at 465 nm (strong), 610 nm (small). This indicates the green and blue fluorescence emission spectra. Emission is associated with defects emerging during the growth of crystallites and one related to deformation of crystallinity due to dislocations and vacancies. The band gap energy () is calculated from the formula

$$E_g = h\nu$$

where, $\nu = c/\lambda$, λ is the wavelength, C is the velocity of light (3×10^8 m/s) and h is the plank's constant 6.626×10^{-34} Js. The calculated band gap energy value is $= 2.67$ eV.

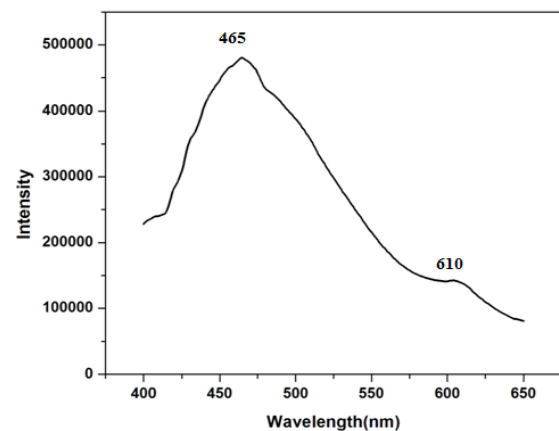


Fig. 10. Emission spectrum of ADLMA crystal.

4. Conclusion

The nonlinear optical ADLMA single crystals were synthesized and grown by slow evaporation technique at room temperature and compared with reported acenaphthene crystal studies. In X-ray diffraction pattern, the well defined Bragg's peak at specific 2θ values confirms the crystallinity of the grown crystals, the additional peak around 21° confirms the addition of DL-malic acid with acenaphthene. The microscopic structural parameters were calculated for prominent peak values. The FTIR spectra illustrated that the presence of characteristic absorption bands are due to the presence of various functional groups in grown NLO crystal. The additional modes of vibrations in FTIR spectrum reveals that the introduction of DL-malic acid in the acenaphthene molecular structure. UV-Vis absorption analysis reveals the electron transition around wavelength 295 nm which confirms the formation of charge transfer in grown crystal. The extended transparency beyond 320 nm says that ADLMA having better transparency than acenaphthene, which is the desired property for various NLO applications. SHG efficiency of grown ADLMA crystal (66 mV) was found to be 3.5 times greater than that of KDP (18 mV) and ANP (19mV). The enhancement of SHG efficiency in ADLMA is due to the addition of DL-

malic acid with acenaphthene. Low value of dielectric loss at high frequencies for grown crystals suggests that the grown crystals possess good optical quality. TG/DTA curves of ADLMA indicated that melting point of ADLMA is 148^oC. Photoluminescence spectra revealed both blue and green fluorescence emission. The chemical composition in ADLMA was verified through elemental analysis. All these studies reveal that the presence of DL-malic acid in ADLMA plays a vital role in improving the linear, nonlinear optical activities and thermal properties of the ADLMA crystals and thus considered as potential candidates for the fabrication of optoelectronic, and nonlinear optical devices.

Acknowledgments

The author expresses their thanks to Prof. P. K. Das (Department of Inorganic and Physical Chemistry IISC, Bangalore), helped for the measurement of Powder SHG efficiency. The authors also revealed their thanks to Dr. Vargeesh Sophisticated Test and Instrumentation Centre (STIC), Cochin for providing instrumentation support.

References

- [1] D. Xu, M.H. Jiang, Z.S. Shao and X.T. Tao. *Synth. Cryst.* **16**, 1 (1987)
- [2] G.C. Xing, M.H. Jiang and Z.S. Shao. *Chinese Phys. Laser.* **14**, 1 (1987)
- [3] H.O. Marcy, L.F. Warren, M.S. Webb, C.A. Ebbers, S.P. Velsko, G.C. Kennedy, G.C. Catella, *Appl. Opt.* **31**, 5051 (1992)
- [4] T. Verbiest, S. Houbrechts, M. Kauranen, K. Clays, A. Persoons, *J. Mater. Chem.* **7**, 2175 (1997)
- [5] P.A. Angeli, S. Dhanushkodi, *Cryst. Res. Tech.* **36**, 1231 (2001)
- [6] X.Q. Wang, D. Xu, D.R. Yuan, Y.P. Tian, W.T. Yu, S.Y. Sun, Z.H. Yang, Q. Fang, M.K. Lu, Y.X. Yan, F.Q. Meng, S.Y. Guo, G.H. Zhang, M.H. Jiang, *Mater. Res. Bull.* **34**, 1999 (2003)
- [7] L. Mariappan, A. Kandasamy, M. Rathnakumari, P. Sureshkumar, *J. of Optik.* **124**, 2630 (2013).
- [8] RW. Munn, CN. Ironside, *Principles and applications of nonlinear optical materials*, London, 1993.
- [9] R. Ramesh babu, N. Balamurugan, N. vijayan, *J. of Cryst. Growth.* **285**, 649 (2005)
- [10] Leena Sinha, Onkar Prasad, Vijaya Narayan, *J. of molecular chem.* **958**, 330 (2010)
- [11] William kemp, *organic spectroscopy*, 1991.
- [12] Anie Roshan, S. Joseph, C. Ittyachen, M.A., *Mater. Lett.* **49**, 299 (2001).
- [13] SK. Kurtz, TT. Perry. *J. of Appl. Phys.* **39**, 3798 (1968)
- [14] Zukowski, P.W. Kantorow, S.B. Aczka, D. Stelmakh, V.F. *Phys. Stat. Sol.* **A112**, 695 (1989).
- [15] U. Von Hundelshausen, *Phys. Lett.* **34A**, 7 (1971)
- [16] C. Balarew, R. Duhlev. *J. Solid Sate Chem.* **55**, 1 (1984)

*Corresponding author: rbkrys@gmail.com